DALTON
FULL PAPER

Mapping charged silver(I) adenine polymers, $[Ad_x + Ag_y - zH]^{(y-z)+}$, *via* electrospray ionization tandem mass spectrometry experiments†

Ana K. Vrkic, Thomas Taverner and Richard A. J. O'Hair*

School of Chemistry, University of Melbourne, Victoria 3010, Australia.
E-mail: rohair@unimelb.edu.au

Received 12th July 2002, Accepted 9th August 2002
First published as an Advance Article on the web 11th October 2002

Electrospray ionization mass spectrometry of solutions containing adenine [or various methylated derivatives] (M) and $AgNO_3$ yields polymeric $[M_x + Ag_y - zH]^{(y-z)+}$ species. The stoichiometry, collision-induced dissociation fragmentation pathways, and ion–molecule reactions with H_2O, CH_3OH, CH_3CN, $BuNH_2$, and pyridine for the adenine– and 1-methyladenine–silver complexes are consistent with model polymeric structures that comprise of $[M_2Ag_2]$ closed "dimers". The $[(adenine)_2Ag_2]$ subunits involve N(3) and N(9) complexation and are linked *via* a bridging silver ion at the N(7) position. In contrast, the results from the 6-*N*,*N*-dimethyladenine–silver complexes are more consistent with a "linear model" polymeric structure. Other methylated adenine systems give different types of mass spectra, depending on the site of methylation. Maps in which the types of $[M_x + Ag_y - zH]^{(y-z)+}$ polymer ions observed are generated as a function of M (where M_x = number of adenine or methyladenine units) *versus* the number of silver ions highlight those systems which follow the "linear model" for polymeric ions and those which do not.

Introduction

Interest in the interactions between biological molecules such as DNA and proteins and bare metal ions and metal complexes continues unabated.[1] Apart from traditional approaches such as X-Ray crystallography and NMR techniques, electrospray ionization mass spectrometry (ESI/MS) has emerged as a powerful new tool in bioinorganic chemistry.[2] Aside from the obvious analytical benefits of providing information on the stoichiometries of complexes,[3] in some instances, information on binding sites can be obtained using tandem mass spectrometry.[4] The emerging area of gas-phase supramolecular chemistry is also a beneficiary of ESI[5] and several recent studies have provided evidence for clusters of small biomolecules with intriguing structures. Examples include alkali metal-induced "self assembly" of the homochiral serine octamer clusters $[(Ser)_8n + n\mathrm{Na}]^{n+}$,[6a] octameric clusters of guanosine $[(Guo)_8 + M]^+$,[6b] and tetrameric clusters of guanine $[(G)_4 + M]^+$.[6c] In all three cases, hydrogen bonding has been implicated in the special clusters observed *via* ESI/MS. As part of an ongoing effort to understand the interactions between metal complexes and small biomolecules and model systems, we have turned our attention to the silver(I) ion, which exhibits a diverse and interesting bio-inorganic chemistry. Examples include its interactions with amino acids, peptides, and amines[7] in the gas phase and its ability to form polymeric structures with nucleobases such as adenine (**A**) in the condensed phase.[8,9]

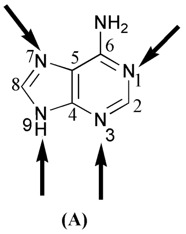

(A)

In solution-phase studies, the adenine residue (in adenosine) has been found to provide three potential metal binding sites, namely N(1), N(3) (occasionally), and N(7).[10] In duplex DNA, the known sites for cation coordination are mainly the N(7) atoms of purines, with the N(1) position of adenine being blocked by hydrogen bonding.[10] Preferential binding of metal cations to the N(7) position has been confirmed *via ab initio* calculations at the Hartree–Fock (HF) level of theory,[11] and by various crystallographic[12a,b] and Raman spectroscopic studies.[12c] Other investigations have also shown that, in addition to binding at the N(7) position, N(1) can be simultaneous occupied by either a proton[13a] or a second metal ion.[13b]

X-Ray crystallographic studies have demonstrated that adenine and its derivatives can adopt different polymeric structures with Ag^+, including the di-μ-adeninium disilver(I) perchlorate monohydrate structure (**B**)[8a] and infinite cationic polymeric chains of 9-methyladenine complexed with silver ions (**C**).[8b] The former structure contains planar centrosymmetric $[(adeninium)_2Ag_2]^{4+}$ cations, in which two adjacent silver atoms are bridged by two N(3),N(9)-bidentate adeninium cations, where N(1) is protonated and the acidic proton originally attached to N(9) is displaced to N(7).[8a] In the latter structure, each 9-methyladenine acts as a bridging bidentate ligand *via* N(1) and N(7), while each Ag cation is co-ordinated to N(1) of one ligand and N(7) of the next ligand in the chain.[8b]

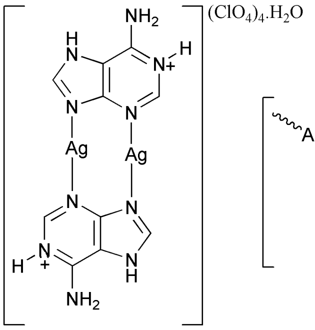

(B)

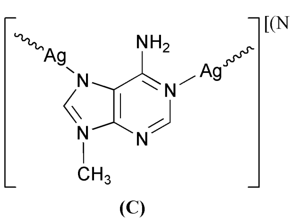

(C)

---

† Gas-phase ion chemistry of biomolecules. Part 33.[27]

Electronic supplementary information (ESI) available: Fig. S1–3, discussed in the text. See http://www.rsc.org/suppdata/dt/b2/b206824a/

4024 *J. Chem. Soc., Dalton Trans.*, 2002, 4024–4034 DOI: 10.1039/b206824a

A number of solution-phase studies have also examined the nature of binding between adenine and its derivatives with Ag(I).[9,14] In these instances, evidence for long, linear polymeric adenine–silver complexes were reported in crystallographic[9a] and flow linear dichroism studies.[9b] The formation of adenine–silver complexes have also been thoroughly investigated by potentiomeric titration experiments, in which various insoluble precipitates were formed in 1:1 and 3:2 (silver:adenine) stoichiometries.[9c,14] A more recent study involving the use of UV and IR dichroic spectra has shown that while adenine forms linear (1:1) polymers with silver ions through N(9)–Ag^+–N(9), N(1)–Ag^+–N(1), and/or N(9)–Ag^+–N(1) bonding, it most likely degrades into dimers as the molar ratio of silver to adenine is increased. Results using these techniques also suggest that the 1-methyladenine–silver complex forms a dimer, $[(1\text{-MeAd})_2\text{-}Ag_2]$, in which the amino proton is replaced by silver and there is simultaneous coordination of the silver to the N(7) nitrogen of a second 1-methyladenine, as shown in structure (**D**).[14g]

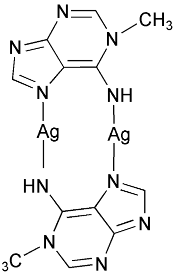

(D)

Given the diversity of structures observed from adenine–silver complexes, in this work, we examine the types of ions formed when mixtures of adenine and silver, or its methylated derivatives, are subjected to electrospray ionization mass spectrometry and tandem mass spectrometry.

Experimental

All experiments were performed using a commercially available quadrupole ion trap mass spectrometer (Finnigan-MAT model LCQ, San Jose, CA) equipped with electrospray ionization (ESI) and recently modified to allow the introduction of neutral reagents *via* the helium background gas inlet line.[15] 9-Methyladenine was synthesized *via* standard literature procedures[16] and all other compounds and reagents used were commercially available and used without further purification.

A 1:2 mixture of adenine and silver nitrate was dissolved in a 50:50 mixture of H_2O and CH_3OH (1% acetic acid) (0.1 mg mL^{-1}) and introduced to the mass spectrometer at 3.0 μL min^{-1} *via* electrospray ionization. Typical ESI conditions used were: spray voltage, 4.5–5.5 kV; capillary temperature, 200 °C; nitrogen sheath pressure, 40 psi; capillary voltage/ tube lens offset, 0–10 V. Collision-induced dissociation (CID) of $[M_x + Ag_y - zH]^{(y-z)+}$ ions was carried out by mass selecting the major isotope ions from the Ag isotopic clusters with a 5–10 Th window and subjecting them to the following typical conditions: activation amplitude, 0.35–0.60 V; activation (*Q*), 0.25 V; activation time, 100 ms.

Ion–molecule reactions (IMR) were carried out as previously described.[15] Briefly, once a stable ESI ion signal was obtained, the neutral reagents were introduced into the trap as a part of the helium bath gas. A constant flow of the reagent (5–15 μL h^{-1}) was established using a syringe pump with the syringe needle directed into a measured flow of helium (850–2050 mL min^{-1}). The majority of the gas exits through a flowmeter, whereas a small amount (~1 mL min^{-1}) is drawn into the trap. The LCQ uses a constriction capillary to control the helium flow and is designed to maintain 1.75 mTorr in the trap when 3 psi of He pressure is applied to the capillary. In the stock system, the 3 psi is maintained by an internal regulator that steps down the 40 psi of He that is delivered at the external port. To avoid the dead volume in the internal regulator, we bypass it and deliver the He mixture (3 psi) directly to the capillary. This greatly decreases the lag time after changes in reagent concentration.[17]

Results and discussion

(A) Formation of $[Ad_x + Ag_y - zH]^{(y-z)+}$ ions under ESI/MS conditions

Fig. 1 shows the electrospray ionization mass spectrum of a 50:50 methanol–water (1% acetic acid) 1:2 mixture of adenine and silver nitrate. It is immediately apparent that a range of polymeric species are present, some with greater ion intensities (*e.g.* $[Ad_2 + Ag_2 - H]^+$ *m*/*z* 485) than the neighbouring species, suggesting a greater degree of stability. The ions formed under ESI/MS conditions are all even-electron species conforming to the general formula $[Ad_x + Ag_y - zH]^{(y-z)+}$. While singly charged ions are generally observed (*i.e.* $y - z = 1$), several doubly charged ions were also noted. The most abundant doubly charged species is the $[Ad_2 + Ag_2]^{2+}$ ion, followed by the $[Ad_6 + Ag_8 - 6H]^{2+}$, $[Ad_8 + Ag_{10} - 8H]^{2+}$, and $[Ad_8 + Ag_{12} - 10H]^{2+}$ ions. The observation of doubly charged ions is highly dependent on the ESI source conditions, which can be tuned to maximize the abundance of specific ions. The stoichiometries of the various complexes and their relative abundances suggest that these complexes exhibit "cluster" formation, in which a dimeric species related to (**B**) plays a key role, as opposed to a linear structure. To further probe this notion, both the effects of methylation on the adenine ring, as well as the fragmentation patterns and the ion–molecule reactions of these complexes, were examined. The results of these studies are discussed in detail in sections B–D and our overall conclusions regarding the structures of these systems are discussed in section E.

(B) Effects of methylation of adenine on the observation of polymeric ions under ESI/MS conditions

In order to gain a more comprehensive understanding of the type of binding that was occuring in the $[Ad_x + Ag_y - zH]^{(y-z)+}$ system, various methylated adenine derivatives were mixed with $AgNO_3$ and subjected to ESI/MS to observe how methylation of the adenine ring effects the formation of polymeric ions. The ESI/MS of the Ag(I)–6-*N*,*N*-dimethyladenine (**E**) system displayed a number of similarities to adenine–silver in the lower mass range region [Fig. 1(A) and 2(A)]. In addition to having similar relative abundances for the major types of complexes {particularly $[DMA_2 + Ag_2 - H]^+$ *m*/*z* 541, which was the base peak (DMA = 6-*N*,*N*-dimethyladenine)}, the doubly charged dimer ion $[DMA_2 + Ag_2]^{2+}$ *m*/*z* 271 was also clearly observed, as with the adenine–silver system. An examination of the higher mass regions of the two spectra, however, revealed that although the $[(Ad/DMA)_4 + Ag_5 - 4H]^+$ and $[(Ad/DMA)_5 + Ag_6 - 5H]^+$ species dominated both spectra, there was a significant difference in the other types of polymeric species formed in that region [Fig. 1(B) and 2(B)]. The importance of this observation will become evident in section D.

Methylating adenine at the N1 position (**F**) also resulted in the formation of a number of polymeric ions (Fig. 3). From the spectra, it is evident that, in the lower mass range, most of the ions observed are analogous to those observed for the adenine–silver system [Fig. 1(A) and 3(A)]. The most obvious differences between the two spectra are the relative intensities of various complexes, the absence of the doubly charged dimer, and the formation of species involving the nitrate counterion. There is further contrast when comparing the species formed in the higher mass range. Although $[(1 - MeAd)_4 + Ag_5 - 4H]^+$ (*m*/*z* 1133) is still the base peak, there are both some species missing

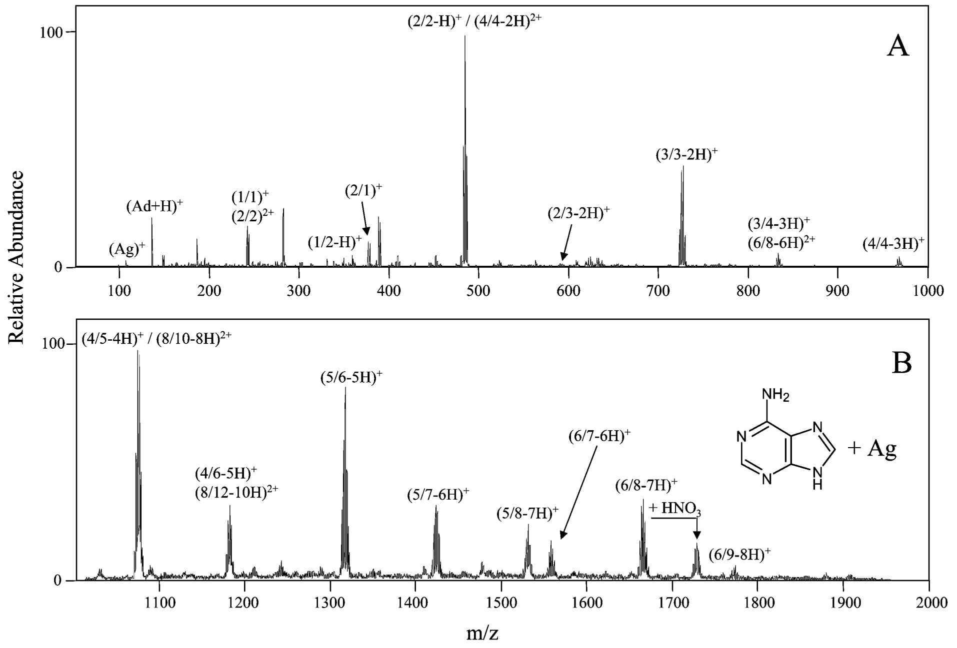

Fig. 1 ESI/MS of a 2:1 solution of $AgNO_3$ with adenine: (a) mass range 50–1000 Th, tuned for ion at *m*/*z* 485 (a combination of $[2/2 - H]^+$ and $[4/4 - 2H]^{2+}$); (b) mass range 1000–2000 Th, tuned for ion at *m*/*z* 1075 (a combination of $[4/5 - 4H]^+$ and $[8/10 - 8H]^{2+}$). Note that $[2/2 - H]^+$ denotes a polymeric ion consisting of $[2\ \text{adenine}/2\ \text{silver} - H]^+$.

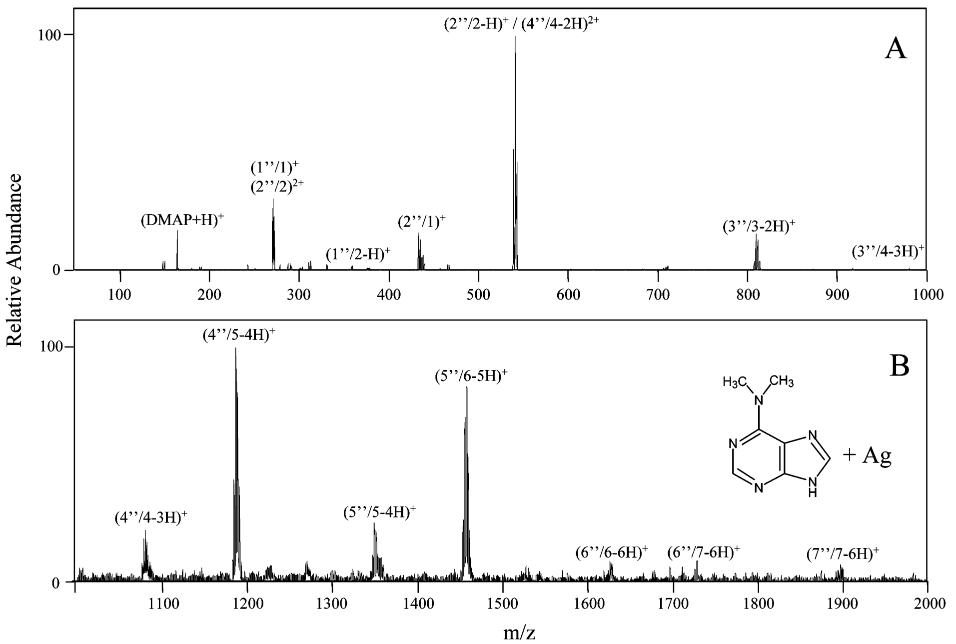

Fig. 2 Electrospray ionization ESI/MS of a 2:1 solution of $AgNO_3$ with 6-*N*,*N*-dimethyladenine: (a) mass range 50–1000 Th, tuned for ion at *m*/*z* 541 (a combination of $[2''/2 - H]^+$ and $[4''/4 - 2H]^{2+}$); (b) mass range 1000–2000 Th, tuned for ion at *m*/*z* 1187 $[4''/5 - 4H]^+$. Note that $[2''/2 - H]^+$ denotes a polymeric ion consisting of [2 (6-*N*,*N*-dimethyladenine)/2 silver − H)]$^+$.

(which were observed for adenine–silver) and some new species not previously seen. The three other monomethylated adenines (**G**–**I**) all yielded similar spectra to each other, with some of the expected polymeric complexes being observed. However, these spectra were consistently weaker and higher mass ions were mostly absent, indicating that the formation of polymeric ions under ESI/MS for these systems was not as favourable as with 1-methyladenine. The most notable absence was that of the $[(MeAd)_2 + Ag_2 - H]^+$ ion, which dominated the other three systems.

To try and account for these differences, it is worthwhile considering the tautomeric forms of these methylated adenines, as they are likely to influence the types of complexes formed. The most stable tautomeric stuctures for 6-*N*,*N*-dimethyladenine (**E**),1-methyladenine (**F**), 3-methyladenine (**G**), 7-methyladenine (**H**), and 9-methyladenine (**I**) are shown below.[18]

Upon inspection of these structures, it is evident that, while 1-methyladenine prefers to exist in the N(9)H imine form, 6-*N*,*N*-, 3-, 7-, and 9-methyladenine all prefer the amine form. Another factor which plays an integral role in determining what types of $[MeAd_x + Ag_y - zH]^{(y-z)+}$ ions are formed is the acidity of the labile protons. Thus, the pK_as of 6-*N*,*N*-, 1-, 7-, and 9-methyladenine are 10.0–10.5, 11.0–11.9, 14.7, and 16.7–17.0, respectively, and show that 6-*N*,*N*-dimethyladenine is the most acidic species, followed by 1-, 7-, and then 9-methyladenine.[19] Experimentally, the ease and intensity with which the $[DMA_x + Ag_y - zH]^{(y-z)+}$ and $[1\text{-}MeAd_x + Ag_y - zH]^{(y-z)+}$ ions were able to form relative to the other methylated adenines,

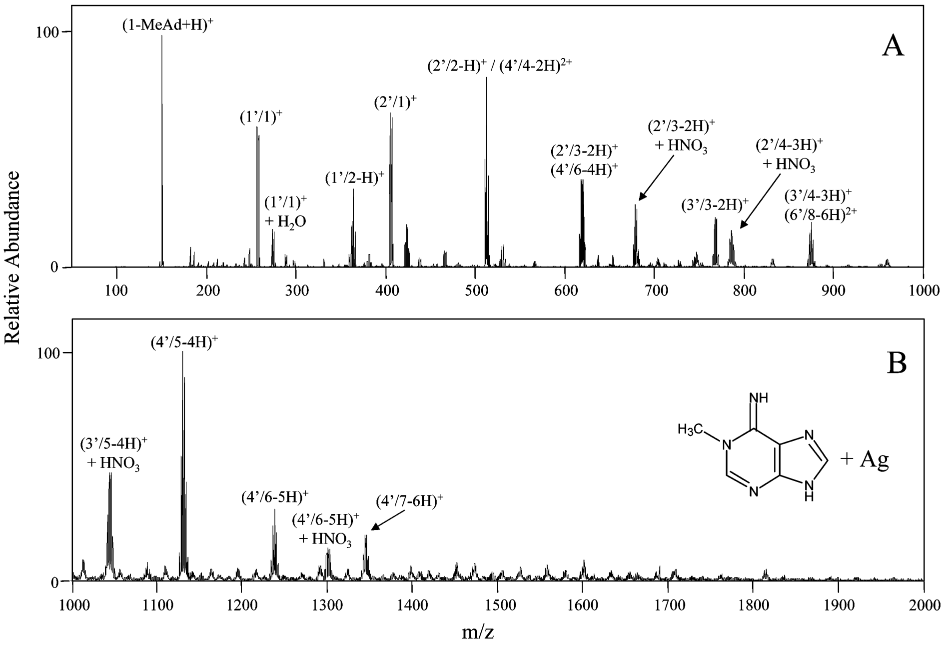

Fig. 3 Electrospray ionization ESI/MS of a 2:1 solution of $AgNO_3$ with 1-methyladenine: (a) mass range 50–1000 Th, tuned for ion at *m*/*z* 513 (a combination of $[2'/2 - H]^+$ and $[4'/4 - 2H]^{2+}$); (b) mass range 1000–2000 Th, tuned for ion at *m*/*z* 1131 $[4'/5 - 4H]^+$. Note that $[2'/2 - H]^+$ denotes a polymeric ion consisting of $[2\ (\text{1-methyladenine})/2\ \text{silver} - H)^+]$.

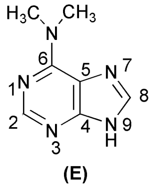

(E)

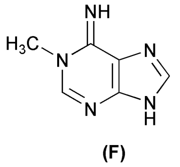

(F)

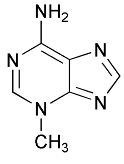

(G)

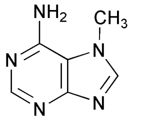

(H)

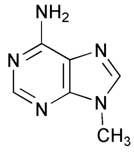

(I)

seems to reiterate the correlation between the acidity of the substituted adenine and the type/number of complexes formed. Another factor which influences the types of species formed is the position of the methyl substituent. Previously, it was noted that the $[(MeAd)_2 + Ag_2 - H]^+$ ion was absent from the 3-, 7-, and 9-methyladenine–silver spectra. As methyl substitution at the N(3) and N(9) would preclude dimer formation, this observation offers further evidence of possible dimer formation [involving metal complexation at N(3) and N(9)] for the adenine–silver complexes.

(C) Fragmentation reactions of ions under CID MS^n conditions

Each of the ions in Fig. 1, 2, and 3 can be mass selected and its gas-phase fragmentation reactions studied under collision-induced dissociation (CID) conditions. Our aim was to see if such data could provide clues as to the structural features of these polymer ions. An additional bonus is that it may be possible to generate new silver adenine complexes not present in the conventional ESI/MS. Tables 1, 2, and 3 list the predominant dissociation pathways for the adenine–silver, 6-*N*,*N*-dimethyladenine–silver and 1-methyladenine–silver systems. Note that, in these tables, MS^n refers to the stages of mass analysis associated with various steps of ion isolation and subsequent CID (*e.g.* MS^3 = MS/MS/MS and involves two CID steps).

Upon inspection of Tables 1, 2, and 3, it is immediately apparent that a diverse set of fragmentation reactions are observed, ranging from losses of simple silver species to fragmentation involving losses of silver bonded to adenine. The former reactions can be classified into three groups: (1) formation of the silver ion, as illustrated for the $[M + Ag]^+$ ion of adenine (Table 1 and eqn. 1); (2) loss of a neutral silver atom, which results in the formation of a radical cation, as illustrated for the $[M + Ag]^+$ ion of 1-methyladenine (Table 3 and eqn. 2); (3) loss of silver hydride, $(AgH)^0$, as illustrated for the $[M + Ag]^+$ ion of 6-*N*,*N*-dimethyladenine (Table 2 and eqn. 3). The latter losses are more interesting from a structural perspective, since it may be possible to distinguish between various possible polymeric structures, as discussed for specific examples below.

$$[M + Ag]^+ \longrightarrow Ag^+ + M \qquad (1)$$

$$[M + Ag]^+ \longrightarrow M^{+\bullet} + Ag \qquad (2)$$

$$[M + Ag]^+ \longrightarrow [M - H]^+ + AgH \qquad (3)$$

One of the first examples to illustrate the subtle differences in fragmentation between the three systems are the $[M_2 + Ag_3 - 2H]^+$ ions. The MS/MS spectra of these complexes are shown in Fig. 4(a) (where M = adenine), (b) (where M = 1-methyladenine), and (c) (where M = 6-*N*,*N*-dimethyladenine), respectively. It should be noted that Fig. 4(c) results from an MS^3 experiment in which the $[M_2 + Ag_3 - 2H]^+$ ion is synthesized from the $[M_3 + Ag_3 - 2H]^+$ precursor ion. This approach was adopted because it yielded the strongest CID spectrum. Additionally, the symbolism of Cooks and co-workers will be used to denote mutistage/multi reaction events for the MS^n experiments.[20] Each mass selection event is indicated by a solid circle with the mass of the selected ion being listed to the right and with a connecting arrow to either a scanning mass analysis event (indicated by an open circle) or a further mass isolation event.

Clearly, the three sets of spectra are quite different: while neutral adenine loss is observed to be the main primary fragmentation pathway for $[Ad_2 + Ag_3 - 2H]^+$, dimer loss is observed as the predominant dissociation pathway for $[(\text{1-MeAd})_2 + Ag_3 - 2H]^+$, with no sign of 1-methyladenine loss at all. For $[DMA_2 + Ag_3 - 2H]^+$ however, loss of silver hydride is seen as the main fragmentation pathway. In order to discern

Table 1 Major fragmentation pathways of $[Ad_xAg_y - zH]^{(y-z)+}$ ions under CID conditions

	Main CID products[a]						Expected and observed no. of adducts[b]						
Complex	MS^n	$-Ag^0$	$-Ad^0$	$-[Ad + Ag - H]^0$	$-[Ad_2 + Ag_2 - 2H]^0$	Other major product ions[c]	I	II	III	IV	V	VI	VII
$[Ad + Ag]^+$	3	—	100	—	—	—	1	1	1,1	1	1	1	1
$[Ad_2 + Ag]^+$	2	—	100	—	—	—	0	0	0	0	0	0	0
$[Ad + Ag_2 - H]^+$	2	100	—	—	—	—	2	2	2,1	2	2	2	2
$[Ad_2 + Ag_2]^{2+}$	2	—	—	—	—	$-[1,1]^+$ (100)	1	0	2,2	2	2	2	2
$[Ad_2 + Ag_2 - H]^+$	2[d]	—	100	6	—	—	1	0	0	0	0	1	1
$[Ad + Ag_3 - 2H]^+$	3	100	—	—	—	—	N/A	3	3,2	2	3	3	3
$[Ad_2 + Ag_3 - 2H]^+$	2	—	100	33	—	—	2	1	1,1	1	1	1	1
$[Ad_3 + Ag_3 - 2H]^+$	2	—	52	—	100	—	1	0	0	1	1	2	1
$[Ad_2 + Ag_4 - 3H]^+$	3	100[e]	—	—	—	—	N/A	2	1,1	1	2	2	2
$[Ad_3 + Ag_4 - 3H]^+$	2[d]	—	9	3	100	$-[1,2 - 2H]^0$ (10)	2	1	0	0	1	1	1
$[Ad_4 + Ag_4 - 3H]^+$	2	—	31	—	100	—	1	0	0	0	0	1	2
$[Ad_3 + Ag_5 - 4H]^+$	3	—	33[e]	9[e]	49[e]	$-[2,3 - 3H]^0$ (100)[e]	N/A	2	1,1	1	1	1	1
$[Ad_4 + Ag_5 - 4H]^+$	2[d]	—	10	3	100	$-[2,3 - 3H]^0$ (5); $-[3,2 - 2H]^0$ (4)	2	0	0	0	1	1	1
$[Ad_3 + Ag_6 - 5H]^+$	4	100	—	—	—	—	N/A	3	1,1	X	2	2	X
$[Ad_4 + Ag_6 - 5H]^+$	2[d]	—	100	5	60	$-[1,2 - 2H]^0$ (5); $-[2,3 - 3H]^0$ (31); $-[2,4 - 4H]^0$ (3); $-[3,4 - 4H]^0$ (11)	N/A	1	0	0	0	2	2
$[Ad_5 + Ag_6 - 5H]^+$	2	—	60	—	100	$-[3,4 - 4H]^0$ (4)	2	0	0	0	0	1	0
$[Ad_5 + Ag_7 - 6H]^+$	2	—	100	18	9	—	N/A	1	0	0	1	1	1
$[Ad_6 + Ag_7 - 6H]^+$	2	—	—	—	100	—	2	0	0	X	X	X	X
$[Ad_5 + Ag_8 - 7H]^+$	2	—	100	4	39	$-[2,3 - 3H]^0$ (5); $-[3,4 - 4H]^0$ (3)	N/A	2	0	0	0	X	X
$[Ad_6 + Ag_8 - 7H]^+$	2	—	100	—	15	—	N/A	0	0	0	0	X	X
$[Ad_6 + Ag_9 - 8H]^+$	2	—	47	—	100	$-[3,4 - 4H]^0$ (3)	N/A	1	0	X	X	X	X

[a] Abundance (%) relative to the most abundant product ion. [b] I = expected number of coordination sites for linear model; II = expected number of coordination sites for dimer model; III, IV, V, VI, and VII = the observed number of coordinated neutral molecules for background methanol–water, methanol, acetonitrile, butylamine, and pyridine, respectively. [c] With relative abundances ≥ 3%. [d] Ions at higher *m*/*z* than the $[Ad_xAg_y - zH]^{(y-z)+}$ formula are observed, indicative of an overlap with doubly charged ions {*i.e.* $2[Ad_xAg_y - zH]^{2(y-z)+}$}. [e] The adduct is the most abundant product ion. The abundances of these ions are scaled relative to the most abundant fragmentation product. X = experiment not performed. N/A = the stoichiometry of this complex does not allow it to form a linear structure.

Table 2 Major fragmentation pathways of $[DMA_xAg_y - zH]^{(y-z)+}$ ions under CID conditions

	Main CID products[a]						Expected and observed no. of adducts[b]			
Complex	MS^n	$-[Ag + H]^0$	$-M^0$	$-[M + Ag - H]^0$	$-[M_2 + Ag_2 - 2H]^0$	Other major product ions[c]	I	II	III	IV
$[DMA + Ag]^+$	2	100	4	—	—	—	1	1	1,1	1
$[DMA_2 + Ag]^+$	2	—	100	—	—	—	0	0	0	0
$[DMA + Ag_2 - H]^+$	2	100	—	—	—	$-2Ag$ (66)	2	2	1,1	2
$[DMA_2 + Ag_2]^{2+}$	2	—	—	—	—	$-[1,1]^+$ (100)	1	0	2,2	2
$[DMA_2 + Ag_2 - H]^+$	2[d]	—	100	46	—	$-[1'',2]^0$ (6)	1	0	0	0
$[DMA_2 + Ag_3 - 2H]^+$	2	100	—	—	—	—	2	1	1,1	1
$[DMA_3 + Ag_3 - 2H]^+$	2[d]	—	24[e]	5[e]	100[e]	$-[1'',2 - 2H]^0$ (2)[e]	1	0	0	0
$[DMA_3 + Ag_4 - 3H]^+$	3	21	—	1	100	$-[2'',3 - H]^0$ (5)	2	1	0	0
$[DMA_4 + Ag_4 - 3H]^+$	2	—	30	—	100	$-[2'',1 - H]^0$ (15)	1	0	0	X
$[DMA_4 + Ag_5 - 4H]^+$	2	—	—	72[e]	90[e]	$-[2,3 - 3H]^0$ (100)[e]; $-[3,3 - H]^0$ (14)[e]	2	0	0	0
$[DMA_5 + Ag_5 - 4H]^+$	2	—	100	2	80	$-[2,1 - H]^0$ (36); $-[3,2 - 2H]^0$ (2); $-[3,3 - H]^0$ (2)	1	N/A	0	X
$[DMA_5 + Ag_6 - 5H]^+$	2	—	—	—	100	—	2	0	0	0
$[DMA_6 + Ag_6 - 5H]^+$	2	—	76	17	100	$-[2'',1 - H]^0$ (18)	1	N/A	0	X
$[DMA_6 + Ag_7 - 6H]^+$	2	—	—	—	100	—	2	0	0	X

[a] Abundance (%) relative to the most abundant product ion. [b] I = expected number of coordination sites for linear model; II = expected number of coordination sites for dimer model; III and IV = the observed number of coordinated neutral molecules for background methanol–water and methanol, respectively. [c] With relative abundances ≥ 3%. [d] Ions at higher *m*/*z* than the $[DMA_xAg_y - zH]^{(y-z)+}$ formula are observed, indicative of an overlap with doubly charged ions (*i.e.* $2[DMA_xAg_y - zH]^{2(y-z)+}$}. [e] The adduct is the most abundant product ion. The abundances of these ions are scaled relative to the most abundant fragmentation product. X = experiment not performed. N/A = stoichiometry of complex does not allow it to form a dimeric structure.

which types of structure could yield the various fragmentation products, both the "dimer" cluster and linear models were compared against one another (Schemes 1, 2, and 3). It is immediately apparent upon inspection of Scheme 1 that $[Ad_2 + Ag_3 - 2H]^+$ is only able to exist in the dimer cluster form, as the $[Ad + Ag_3 - 2H]^+$ product ion structure is not possible with the "linear-model". Schemes 2 and 3, however, highlight that $[(1\text{-}MeAd)_2 + Ag_3 - 2H]^+$ and $[DMA_2 + Ag_3 - 2H]^+$ can exist

Table 3 Major fragmentation pathways of $[(1\text{-MeAd})_x\mathrm{Ag}_y - z\mathrm{H}]^{(y-z)+}$ ions under CID conditions

	Main CID products[a]							Expected and observed no. of adducts[b]			
Complex	MS^n	$-\mathrm{Ag}^0$	$-[\mathrm{Ag + H}]^0$	$-\mathrm{M}^0$	$-[\mathrm{M + Ag - H}]^0$	$-[\mathrm{M_2 + Ag_2 - 2H}]^0$	Other major product ions[c]	I	II	III	IV
$[1\text{-MeAd} + \mathrm{Ag}]^+$	3	66[e]	—	100[e]	—	—	$-\mathrm{CH_3CN}$ (88)[e]	1	1	1,1	1
$[(1\text{-MeAd})_2 + \mathrm{Ag}]^+$	2	—	—	100	—	—	—	0	0	0	0
$[1\text{-MeAd} + \mathrm{Ag_2} - \mathrm{H}]^+$	3	100[e]	74[e]	—	—	—	$-2\mathrm{Ag}$ (29)[e]	2	2	1,1	0
$[(1\text{-MeAd})_2 + \mathrm{Ag_2} - \mathrm{H}]^+$	2[d]	—	2	100	6	—	—	1	0	0	0
$[(1\text{-MeAd})_2 + \mathrm{Ag_3} - 2\mathrm{H}]^+$	2[d]	—	—	—	100	—	$-[1',2 - 2\mathrm{H}]^0$ (2)	2	1	0	1
$[(1\text{-MeAd})_3 + \mathrm{Ag_3} - 2\mathrm{H}]^+$	2	—	—	100	—	—	—	1	0	0	0
$[(1\text{-MeAd})_3 + \mathrm{Ag_4} - 3\mathrm{H}]^+$	2[d]	—	—	—	100	2	—	2	1	0	0
$[(1\text{-MeAd})_4 + \mathrm{Ag_4} - 3\mathrm{H}]^+$	2	—	—	100	—	1	$-[2',1 - \mathrm{H}]^0$ (6)	1	0	0	X
$[(1\text{-MeAd})_3 + \mathrm{Ag_5} - 4\mathrm{H}]^+$	2[d]	100	—	63	24	—	$-[1',2 - 2\mathrm{H}]^0$ (59); $-[2',3 - 3\mathrm{H}]^0$ (4)	N/A	2	0	2
$[(1\text{-MeAd})_4 + \mathrm{Ag_5} - 4\mathrm{H}]^+$	2	—	—	25	20	100	$-[3',3 - 3\mathrm{H}]^0$ (3)	2	0	0	0

[a] Abundance (%) relative to the most abundant product ion. [b] I = expected number of coordination sites for linear model; II = expected number of coordination sites for dimer model; III and IV = the observed number of coordinated neutral molecules for background methanol–water and methanol, respectively. [c] With relative abundances ≥ 3%. [d] Ions at higher *m*/*z* than the $[1\text{-MeAd}_x\mathrm{Ag}_y - z\mathrm{H}]^{(y-z)+}$ formula are observed, indicative of an overlap with doubly charged ions {*i.e.* $2[1\text{-MeAd}_x\mathrm{Ag}_y - z\mathrm{H}]^{2(y-z)+}$}. [e] The adduct is the most abundant product ion. The abundances of these ions are scaled relative to the most abundant fragmentation product. X = experiment not performed. N/A = stoichiometry of complex does not allow it to form a linear structure.

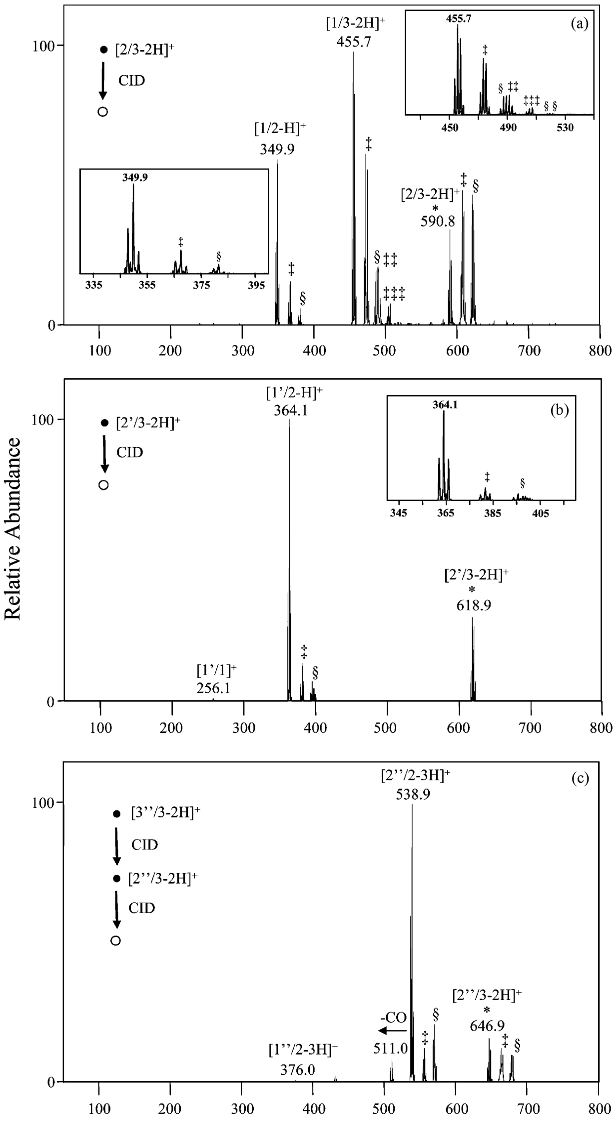

Fig. 4 LCQ CID MS/MS of the $[2/3 - 2\mathrm{H}]^+$ ion of (a) adenine, (b) 1-methyladenine, and (c) 6-*N*,*N*-dimethyladenine. Note that adducts with background water or methanol are denoted as ‡ and §, respectively.

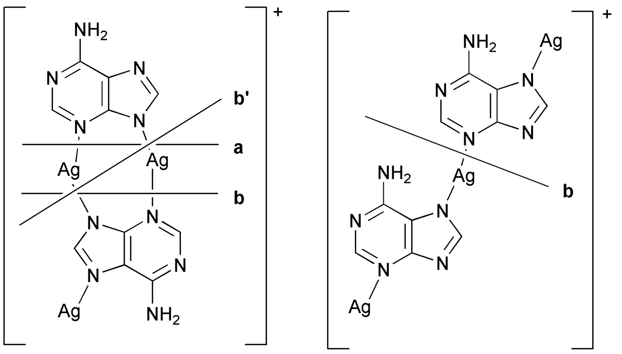

Formation of [Ad+3Ag-2H]+ (i.e. loss of Ad (a)) is not possible with a linear model.

Scheme 1 a = Loss of Ad, b = loss of $[\mathrm{Ad + Ag - H}]^0$, b′ = loss of an alternative isomer of $[\mathrm{Ad + Ag - H}]^0$.

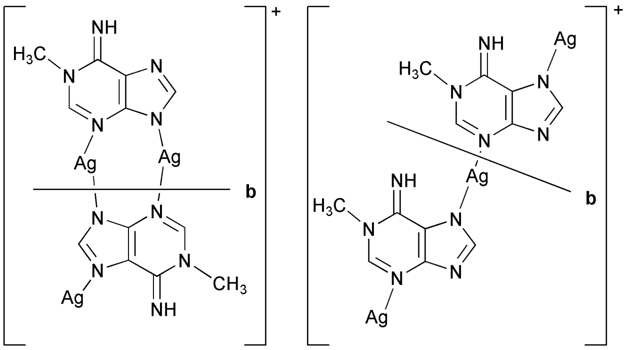

Scheme 2 b = Loss of $[1\text{-MeAd} + \mathrm{Ag - H}]^0$.

as either type of structure, which cannot be distinguished based on the fragmentation reactions observed. The type of bonding shown for (1-MeAd) + Ag in structure (**D**) can also be considered as a distinct possibility in this case as well.

Fig. 5 shows the CID of the $[\mathrm{Ad_3 + Ag_3} - 2\mathrm{H}]^+$ and $[(1\text{-MeAd})_3 + \mathrm{Ag_3} - 2\mathrm{H}]^+$ ions for comparison and, once again, we see a major difference between the fragmentation of the two species. For $[\mathrm{Ad_3 + Ag_3} - 2\mathrm{H}]^+$, dimer loss is observed to be the predominant dissociation pathway, while for $[(1\text{-MeAd})_3 + \mathrm{Ag_3} - 2\mathrm{H}]^+$, neutral 1-methyladenine loss is observed. For $[\mathrm{Ad_3 + Ag_3} - 2\mathrm{H}]^+$, note that both the dimer and

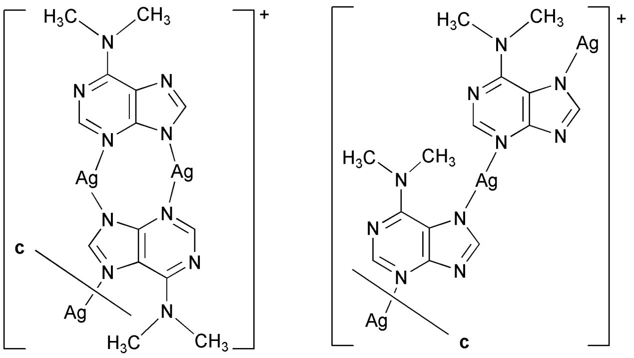

Scheme 3 c = Loss of Ag.

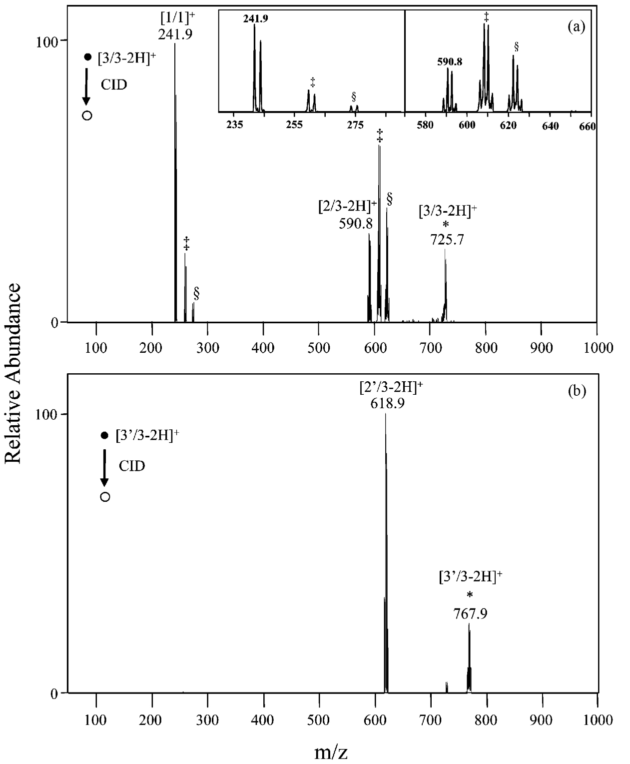

Fig. 5 LCQ CID MS/MS of the [3/3 − 2H]$^+$ ion of (a) adenine and (b) 1-methyladenine. Note that adducts with background water or methanol are denoted as ‡ and §, respectively.

linear models could yield the observed products as shown in Scheme 4. In a similar fashion, both the linear and dimer models could give rise to the loss of 1-methyladenine from [(1-MeAd)$_3$ + Ag$_3$ − 2H]$^+$ (Scheme 5).

One final example which illustrates the differences between these systems is the [M$_5$ + Ag$_6$ − 5H]$^+$ ion (where M = adenine and DMA). CID of the [Ad$_5$ + Ag$_6$ − 5H]$^+$ and [DMA$_5$ + Ag$_6$ − 5H]$^+$ ions [Fig. S1(a) and (b), respectively, ESI] show a striking difference. While dimer loss is the major fragmentation pathway in both instances, neutral adenine loss and dimer formation are observed for [Ad$_5$ + Ag$_6$ − 5H]$^+$, but not for [DMA$_5$ + Ag$_6$ − 5H]$^+$. The formation of the [Ad$_5$ + Ag$_6$ − 5H]$^+$ ion means that the adenine–silver complexes must adopt the "dimeric" cluster structure, as this ion is not possible with the "linear model" (as was the case with [Ad + Ag$_3$ − 2H]$^+$). Consequently, the 6-*N*,*N*-dimethyladenine–silver system appears to possess a linear structure.

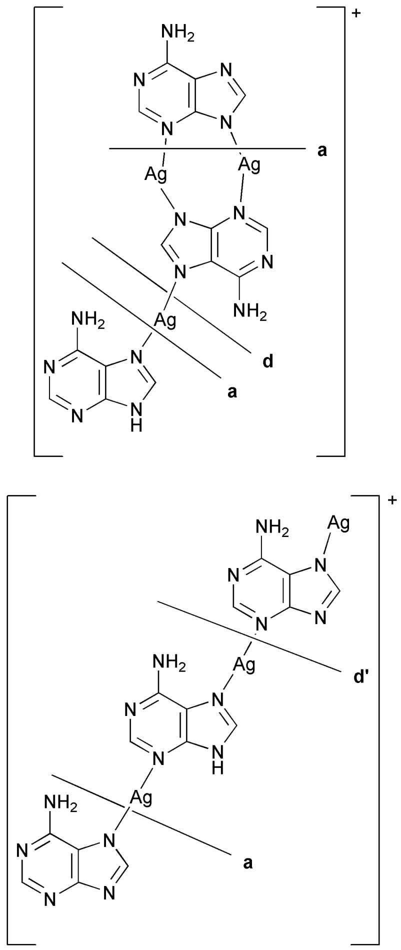

Scheme 4 a = Loss of Ad, d = loss of [Ad$_2$ + Ag$_2$ − H]^0, d' = loss of an alternative isomer of [Ad$_2$ + Ag$_2$ − H]^0.

(D) Formation of adducts *via* ion–molecule reactions as a further structural probe

It is interesting to note that a number of these species undergo ion–molecule reactions (IMR) with background water and methanol. Rather than being regarded as a nuisance, these reactions can potentially offer useful insights into the number of vacant coordination sites on the silver(I) ions present in the complexes, which are known from previous gas-phase studies to prefer to coordinate two ligands.[21] Vachet and co-workers,[22] and others[15] have used ion–molecule reactions of metal complexes to "titrate" the number of vacant coordination sites. Other studies in which water and methanol adducts have been observed include certain binary complexes composed of Ag$^+$ ions and neutral amino acids,[23a] ternary Cu–ligand complexes with amino acids,[23b] and aluminium oxide anion species within an ion trap.[23c] The formation of water–methanol adducts in our experiments can be attributed to these solvents being present as contaminants in the ion-trap bath gas, and thus they can react with the Ag$^+$–adenine complexes upon isolation and collision-induced dissociation. Furthermore, with our modified ion trap, we can add any neutral ligand to the helium bath gas to examine whether it coordinates to a metal complex.[15a]

Fig. 6 predicts how the addition of neutral ligands *via* gas-phase ion–molecule reactions can be used to gain information about the number of silver ions which are coordinatively unsaturated within a number of simple [Ad$_x$ + Ag$_y$ − *z*H]$^{(y-z)+}$ complexes (sites of addition are indicated by bold arrows and note that, for a given complex, several isomers are possible). Given that isomeric closed [Fig. 6(d1) and (e1)] *versus* linear [Fig. 6(d2) and (e2)] dimer structures can, in principle, be distinguished *via* their IMR with neutral ligands, we have incorporated these predictions in the columns labelled as I and II in Tables 1–3. We now turn our attention to comparing these predictions with the experimental data shown in Table 1. Thus, the [Ad + Ag]$^+$ ion, shown in Fig. 6(a) (note that several isomers are possible), has one vacant coordination site and is observed to complex with one water or methanol molecule [see inset to Fig. 5(a)], as well as only one CH$_3$CN, BuNH$_2$, or

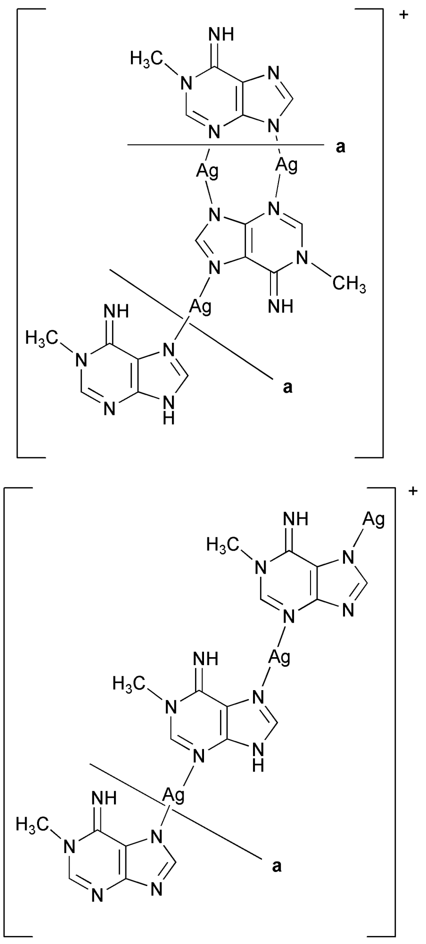

Scheme 5 a = Loss of 1-MeAd.

pyridine ligand (Table 1). In contrast, the $[Ad_2 + Ag]^+$ ion, shown in Fig. 6(b), has no vacant coordination sites and undergoes no IMR with any of the ligands studied (Table 1). The $[Ad + Ag_2 - H]^+$ ion [one possible isomer is shown in Fig. 6(c)] has two vacant coordination sites, both of which are "titrated" by IMR with all of the ligands used (Table 1). The $[Ad + Ag_3 - 2H]^+$ ion [a possible isomer is shown in Fig. 6(f)] has three silver atoms which each posses one vacant coordination site and would be expected to react with up to three background solvent "ligands". A close examination of the water and methanol adducts for the $[Ad + Ag_3 - 2H]^+$ ion reveals that up to three water or two methanol molecules are able to complex to the ion under our experimental conditions [see inset to Fig. 4(a)]. Interestingly, methanol seems to be a poorer coordinating ligand (only coordinates 2 molecules), than nitrogen ligands such as acetontrile, butylamine, and pyridine, which coordinate the expected 3 ligands to the $[Ad + Ag_3 - 2H]^+$ ion (Table 1). The behaviour of the $[Ad_2 + Ag_2]^{2+}$ ion towards neutral ligands in IMR is interesting. In all cases, two ligands are found to complex to this ion, which deviates from the predictions of no ligand addition for the "closed" dimer structure [Fig. 6(d1)] and only one ligand addition for the linear dimer structure [Fig. 6(d2)]. Clearly, the charge on the ion plays a significant role in its IMR with ligands, since the behaviour of the $[Ad_2 + Ag_2 - H]^+$ ion is different to the $[Ad_2 + Ag_2]^{2+}$ ion. Thus, the $[Ad_2 + Ag_2 - H]^+$ ion does not add background water or methanol, and also does not undergo IMR with added methanol or acetonitile, consistent with a closed structure [Fig. 6(e1)] rather than a linear one [Fig. 6(e2)]. This ion, does however form adducts with the stronger bases butylamine and pyridine. A similar analysis of the isomeric complexes in Scheme 4 shows that while the CID fragmentation products can arise from either the "cluster" or linear model, the absence of water and methanol adduct formation for the parent ion, $[Ad_3 + Ag_3 - 2H]^+$, would suggest these complexes adopt the cluster structure in which there are no available coordination sites due its "closed" configuration. A comparison of predicted *versus* experimentally observed ligand addition for the larger complexes listed in Table 1 indicates that reactivity with water and methanol generally diminishes with increasing cluster size. Reactivity with the nitrogen ligands is variable, with some of the larger clusters coordinating to the right number of vacant sites (*e.g.* the $[Ad_2 + Ag_4 - 3H]^+$ ion), others "overcoordinating" (*e.g.* the reactions of the $[Ad_4 + Ag_4 - 3H]^+$ ion with butylamine and pyridine), and, more often, "undercoordinating" (*e.g.* the reactions of the $[Ad_3 + Ag_6 - 5H]^+$ ion). A possible explanation for the "overcoordinating" reactions of the $[Ad_2 + Ag_2]^{2+}$ and $[Ad_2 + Ag_2 - H]^+$ ions is that they form hydrogen-bonded complexes of types (**J**) and (**K**).

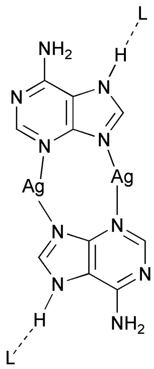

(J)

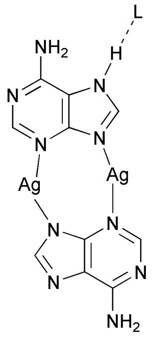

(K)

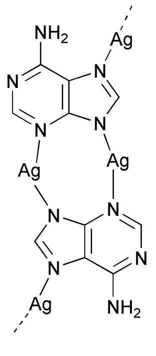

(L)

Although we have not carried out detailed IMR on a wide range of ligands reacting with the complexes involving the methylated adenine systems, we have noted their reactivity towards background water and methanol (Tables 2 and 3). A comparison of the observed ligand additions for the $[M + Ag]^+$, $[M_2 + Ag]^+$, $[M + Ag_2 - H]^+$, and $[M_2 + Ag_2 - H]^+$ ions (where M = 6-*N*,*N*-dimethyladenine and 1-methyladenine respectively), show their behaviour is analogous to that of the adenine–silver system. Furthermore, the reactivity of the larger methylated complexes towards water and methanol is also observed to diminish with increasing cluster size. Thus, it is not possible to infer the exact structure of these methylated species from their ion–molecule reactions with water and methanol.

(E) Possible polymeric structure of the $[xAd + yAg - zH]^{(y-z)+}$ complexes

In an attempt to unify the data presented in sections A–D as arising from a polymer with a repeat unit, we have adopted the approach of Fisher and co-workers, who have mapped the stoichiometries of metal–sulfur ions in mass spectra to infer structures of metal sulfides in the gas phase.[24] Thus, in Fig. 7 we have mapped the types of $[Ad_x + Ag_y - zH]^{(y-z)+}$ polymers observed as a function of the number of adenine units (x axis) *versus* the number of silver ions (y axis). It is important to note that if these $[Ad_x + Ag_y - zH]^{(y-z)+}$ polymers adopt a "linear"-type structure, then the ions observed in the ESI/MS and MS/MS spectra should fall on the region around the X/Y diagonal highlighted on Fig. 7. Any ions which fall outside of this region must have an alternative polymeric structure. Fig. 7 shows the ESI map of the adenine–silver complexes observed in the ion trap, including the ions formed in the initial ESI/MS and from CID reactions. An examination of the map highlights that many of the ions observed for the adenine–silver system fall outside of the linear region. Inspection of their stoichiometries and fragmentation products reveals they are entirely consistent with a "dimeric" cluster model (see further discussion below).

Similar analysis of the maps for the 1-methyladenine–silver complexes and 6-*N*,*N*-dimethyladenine–silver complexes (Fig.

(a) $[Ad+Ag]^+$
1 vacant coordination site:

(b) $[Ad_2+Ag]^+$
No vacant coordination sites:

(c) $[Ad+Ag_2-H]^+$
2 vacant coordination sites:

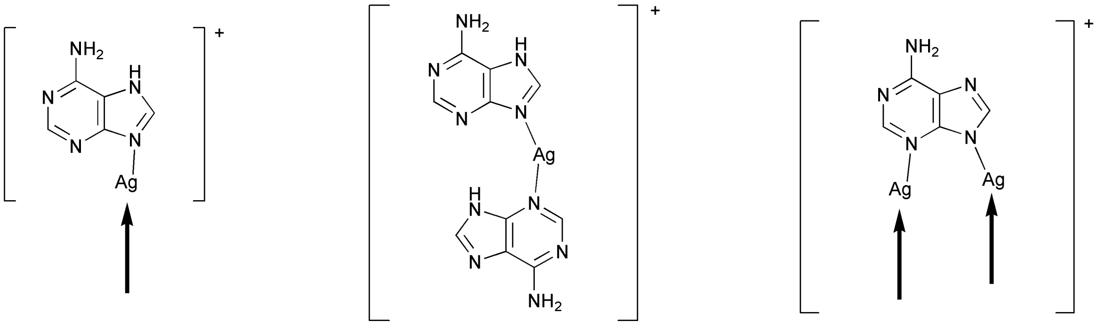

(d1) $[Ad_2+Ag_2]^{2+}$
No vacant coordination sites:

(d2) $[Ad_2+Ag_2]^{2+}$
1 vacant coordination site:

(e1) $[Ad_2+Ag_2-H]^+$
No vacant coordination sites:

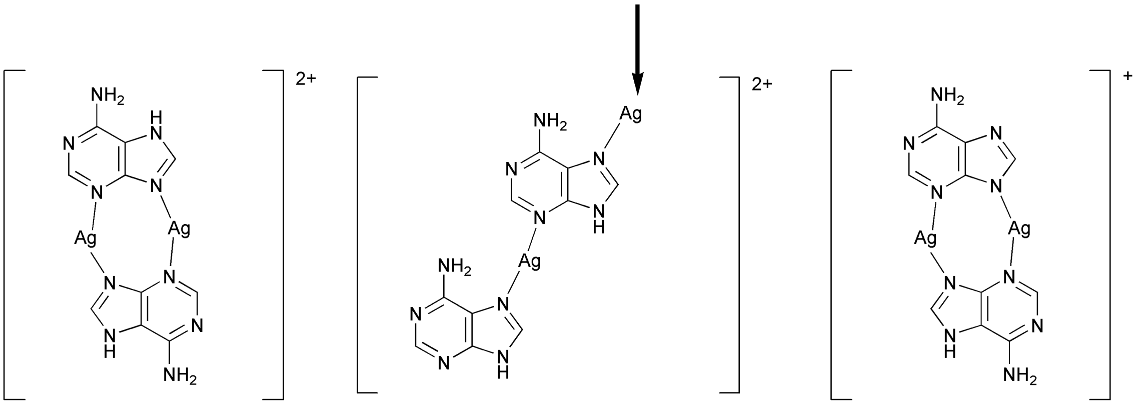

(e2) $[Ad_2+Ag_2-H]^+$
1 vacant coordination site:

(f) $[Ad+Ag_3-2H]^+$
3 vacant coordination sites:

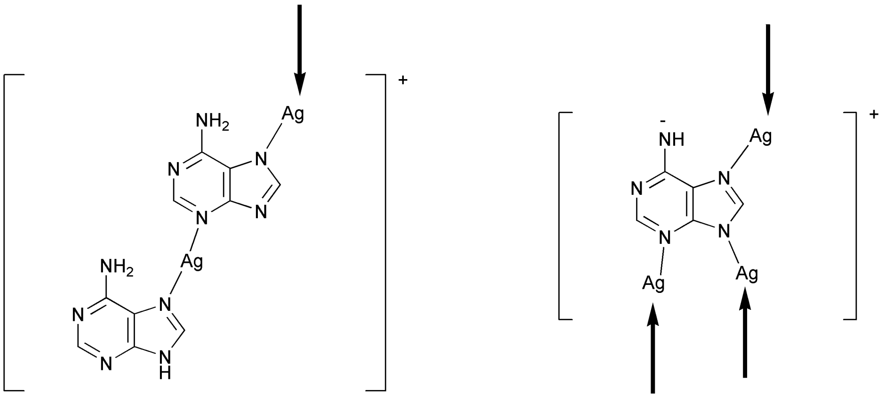

Fig. 6 Possible structures of $[Ad_x + Ag_y - zH]^{(y-z)+}$ ions, showing where solvent molecules such as H_2O and CH_3OH can add to vacant coordination sites.

S2 and S3, ESI) provide a striking contrast, which reaffirms our initial interpretation of the experimental data. It is clear that the 1-methyladenine–silver complexes must adopt some sort of "dimeric" structures as there are species which sit outside the predicted linear region. In direct contrast to this, the 6-*N*,*N*-dimethyladenine–silver system is observed to conform to the "linear" model, as all of its complexes fall within the appropriate region.

From our data as well as the wealth of literature which highlights the formation of dimeric structures involving the bridging of purines *via* metal complexation at N(3) and N(9),[8,25,26] especially the observed X-ray structure (**B**), we propose that the complexes observed in our experiments consist of (adenine$_2$Ag$_2$) subunits [with N(3) and N(9) complexation], that are linked *via* a bridging silver ion at the N(7) positions, as shown in structure (**L**). A quick review of Table 1 reveals that, for the $[Ad_x + Ag_y - zH]^{(y-z)+}$ ions, dimer loss is observed to be one of the primary dissociation pathways, which is consistent the polymeric "dimer" model. Both the stoichiometry and ion–molecule reactions of the complexes just described strongly support the notion that the adenine–silver species adopt structure (**L**). The 1-methyladenine polymeric system may have a related structure or, alternatively, may be composed of dimeric "building block" structures related to structure (**D**).

One important aspect of our proposed model is the formation of special "closed" structures which can be derived from the following formula: $[2n\text{Ad} + (3n - 1)\text{Ag} - (3n - 2)\text{H}]^+$. These species {*i.e.* $[Ad_2 + Ag_2 - H]^+$ (*m*/*z* 485), $[Ad_4 + Ag_5 - 4H]^+$ (*m*/*z* 1075) and $[Ad_6 + Ag_8 - 7H]^+$ (*m*/*z* 1667)} are all more abundant relative to neighbouring species, suggesting they

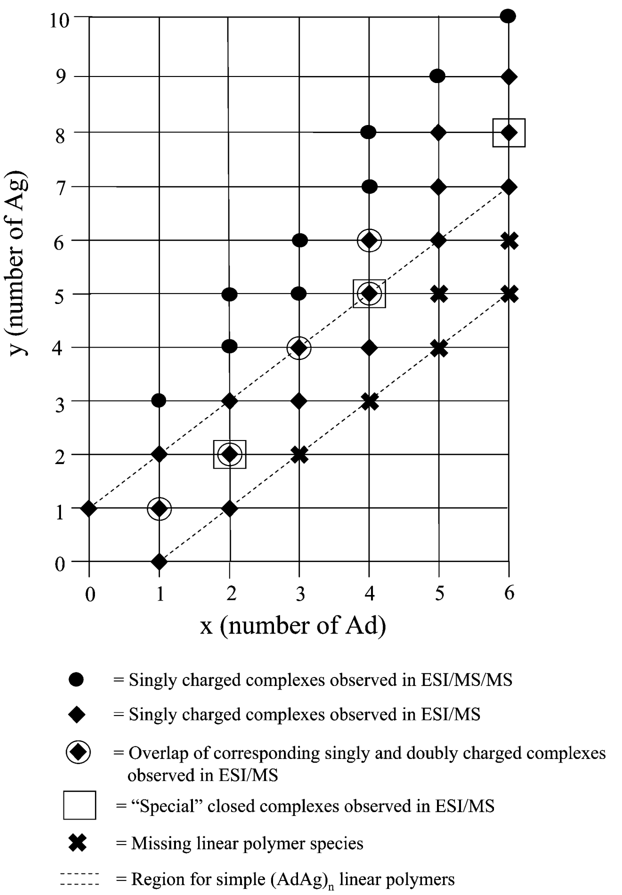

Fig. 7 Map of the $[Ad_x + Ag_y - zH]^{(y-z)+}$ ions observed in the ESI/MS and MS/MS spectra of a 2:1 solution of $AgNO_3$ with adenine in the ion trap. The numbers of adenine and silver ions in each polymer ion are plotted as *x versus y* on the map.

posses a greater degree of stability. It is interesting to speculate that these species are related to the 3:2 (silver:adenine) precipitates (involving a counterion) observed in potentiometric experiments.[9c,14]

Conclusions

By examining the stoichiometry and dissociation pathways of the polymeric species formed for adenine (or various methylated derivatives) (M) and silver and mapping them as the number of adenine *vs.* silver units, it becomes clear which polymers conform to linear and cluster models. Adenine and 1-methyladenine–silver complexes form polymeric structures which consist of $[(M)_2\,(Ag)_2]$ closed "dimers". In our model, the $[(\mathrm{Adenine})_2(Ag)_2]$ subunits involve N(3) and N(9) complexation and are linked *via* a bridging silver ion at the N(7) position. The 6-*N*,*N*-dimethyladenine–silver species, however, conform to a linear model. Overall, there are four main primary fragmentation pathways: (i) loss of silver in the form of either a silver ion, silver atom, or AgH; (ii) loss of neutral adenine; (iii) loss of the neutral "dimer" $[Ad_2 + Ag_2 - 2H]^0$; (iv) loss of the neutral "monomer" $[Ad + Ag\text{–}H]^0$. The preference with which they are lost is dependant upon which adenine species is involved. Differences between the CID products of various adenine species and their methylated analogues highlights that these species adopt varying structures. Ion–molecule reactions between $[M_x + Ag_y - zH]^{(y-z)+}$ ions and neutral ligands can be used to gain insights into vacant coordination sites, although caution should be used, since some complexes can add less than the number expected, while others can add more. Further studies are underway to (i) use DFT calculations to examine the structures and stabilities of the smaller isomeric $[Ad_x + Ag_y - zH]^{(y-z)+}$ ions and (ii) to compare the gas-phase reactivity of novel radical cations formed *via* loss of an Ag atom (*cf.* eqn. 2) with their even-electron counterparts.

Acknowledgements

R. A. J. O. thanks the Australian Research Council for financial support and the University of Melbourne for funds to purchase the LCQ. A. K. V acknowledges the award of a Science Faculty Scholarship (Studentship).

References

1 (*a*) G. L. Eichhorn, *Inorganic Chemistry*, Elsevier-Scientific, New York, 1973, ch. 34; (*b*) H. Lonnberg, *Biocoordination Chemistry*, Horwood, London, 1990, ch. 7; (*c*) A. Siegel and H. Siegel, *Metal Ions in Biological Systems*, Dekker, New York, 1996, vol. 32; (*d*) A. Siegel and H. Siegel, *Metal Ions in Biological Systems*, Dekker, New York, 1996, vol. 33.
2 ESI reviews in bioinorganic chemistry: (*a*) J. L. Beck, M. L. Colgrave, S. F. Ralph and M. M. Sheil, *Mass Spectrom. Rev.*, 2001, **20**, 61; (*b*) Z. Tozuka, *J. Mass Spectrom. Soc. Jpn.*, 2000, **48**, 211; (*c*) J. C. Traeger and R. Colton, *Adv. Mass Spectrom*, 1998, **14**, 637.
3 (*a*) K. A. Johnson, M. F. J. M. Verhagen, P. S. Brereton, M. W. W. Adams and I. J. Amster, *Anal. Chem.*, 2000, **72**, 1410; (*b*) K. A. Johnson and I. J. Amster, *J. Am. Soc. Mass Spectrom.*, 2001, **12**, 819; (*c*) A. M. Bond, R. Colton, A. D'Agostino, J. C. Traeger, A. J. Downard and A. J. Canty, *Inorg. Chim. Acta*, 1998, **267**, 281; (*d*) Y. Hathout, D. Fabris and C. Fenselau, *Int. J. Mass Spectrom.*, 2001, **204**, 1.
4 P. Iannitti-Tito, A. Weimann, G. Wickham and M. M. Sheil, *Analyst*, 2000, **125**, 627.
5 (*a*) C. A. Schalley, *Int. J. Mass Spectrom.*, 2000, **194**, 11; (*b*) C. A. Schalley, *Mass Spectrom. Rev.*, 2001, **20**, 253.
6 (*a*) K. J. Koch, F. C. Gozzo, D. Zhang, M. N. Eberlin and R. G. Cooks, *Chem. Commun.*, 2001, 1854; (*b*) I. Manet, L. Francini, S. Masiero, S. Pieraccini, G. P. Spada and G. Gottarelli, *Helv. Chim. Acta*, 2001, **84**, 2096; (*c*) K. Fukushima and H. Iwahashi, *Chem. Commun.*, 2000, 895.
7 (*a*) V. W.-M. Lee, H. Li, T.-C. Lau, R. Guevremont and K. W. M. Siu, *J. Am. Soc. Mass Spectrom.*, 1998, **9**, 760; (*b*) I. K. Chu, T. Shoeib, X. Guo, F. Rodriquez, T.-C. Lau, A. C. Hopkinson and K. W. M. Siu, *J. Am. Soc. Mass Spectrom.*, 2001, **12**, 163; (*c*) I. K. Chu, X. Guo, T-C. Lau and M. K. W. Siu, *Anal. Chem.*, 1999, **71**, 2364; (*d*) R. N. Grewal, C. F. Rodriquez, T. Shoeib, I. K. Chu, Y.-P. Tu, A. C. Hopkinson and K. W. M. Siu, *Eur. J. Mass Spectrom.*, 2000, **6**, 187.
8 (*a*) C. Gagnon, J. Hubert, R. Rivest and A. L. Beauchamp, *Inorg. Chem.*, 1977, **16**, 2469; (*b*) C. Gagnon and A. L. Beauchamp, *Acta Crystallogr., Sect B*, 1977, **33**, 1448.
9 (*a*) C. Gagnon and A. L. Beauchamp, *Inorg. Chim. Acta*, 1975, **14**, L52; (*b*) Y. Matsuoka, B. Norden and T. Kurucsev, *J. Chem. Soc., Chem. Commun.*, 1984, **23**, 1573; (*c*) K. Gillen, R. Jensen and N. Davidson, *J. Am. Chem. Soc.*, 1964, **86**, 2792.
10 (*a*) H. Sigel, *Chem. Soc. Rev.*, 1993, **22**, 255; (*b*) B. Lippert, *Coord. Chem. Rev.*, 2000, **200–202**, 487.
11 E. H. S. Anwander, M. M. Probst and B. M. Rode, *Biopolymers*, 1990, **29A**, 757.
12 (*a*) E. Sletten and B. Thorstensen, *Acta Crystallogr., Sect. B*, 1974, **30**, 2438; (*b*) E. Sletten and M. Rudd, *Acta Crystallogr., Sect. B*, 1975, **31**, 982; (*c*) B. Giese and D. McNaughton, *J. Phys. Chem. B*, 2002, **106**, 101.
13 (*a*) A. Terzis, *Inorg. Chem.*, 1976, **15**, 793; (*b*) M. J. McCall and M. R. Taylor, *Acta Crystallogr., Sect. B*, 1976, **32**, 1687.
14 (*a*) J. Roemer, *Mikrochim. Acta*, 1977, **2**, 479; (*b*) J. Pouradier and F. Garatin, *C. R. Seances Acad. Sci., Ser. C*, 1977, **284**, 87; (*c*) J. Roemer, *Zentralinst. Kernforsch., Rossendorf Dresden, [Ber] ZfK*, 1974, 82; (*d*) J. Roemer, *Zentralinst. Kernforsch., Rossendorf Dresden, [Ber] ZfK*, 1975, 185; (*e*) J. Roemer, *Mikrochim. Acta*, 1976, **1(2–3)**, 321; (*f*) J. Roemer, *Z. Chem.*, 1975, **15**, 159; (*g*) Y. Matsuoka, B. Norden and T. Kurucsev, *J. Crystallogr. Spectrosc. Res.*, 1985, **15**, 545.
15 (*a*) G. E. Reid, R. A. J. O'Hair, M. L. Styles, W. D. McFadyen and R. J. Simpson, *Rapid Commun. Mass Spectrom.*, 1998, **12**, 1708; (*b*) A. K. Vrkic and R. A. J. O'Hair, *Int. J. Mass Spectrom.*, 2002, **218**, 131.
16 M. Hedayatullah, *J. Heterocycl. Chem.*, 1982, **19**, 249.
17 S. Gronert, *J. Am. Soc. Mass Spectrom.*, 1998, **9**, 845.

18 (*a*) A. B. J. Parusel, W. Rettig and K. Rotkiewicz, *J. Phys. Chem. A*, 2002, **106**, 2293; (*b*) E. S. Kryachko and G. Zundel, *J. Mol. Struct.*, 1998, **446**, 41; (*c*) V. B. Pivovarov, S. G. Stepanian, I. D. Reva, G. G. Sheina and Y. P. Blagoi, *Spectrochim. Acta, Part A*, 1995, **51**, 843; (*d*) K. Schoone, L. Houben, J. Smets, L. Adamowicz and G. Maes, *Spectrochim. Acta, Part A*, 1996, **52**, 383; (*e*) K.-H. Glusenkamp, K. Kruger, G. Eberle, W. Drosdziok, E. Jahde, O. Grundel, A. Neuhaus, R. Boese, P. Stellberg and M. F. Rajewsky, *Angew. Chem., Int. Ed. Engl.*, 1993, **32**, 1640; (*f*) M. Dreyfus, G. Dodin, O. Bensaude and J. E. Dubois, *J. Am. Chem. Soc.*, 1977, **99**, 7027; (*g*) E. L. Stewart, C. K. Foley, N. L. Allinger and J. P. Bowen, *J. Am. Chem. Soc.*, 1994, **116**, 7282; (*h*) A. Broo and A. Holmen, *Chem. Phys.*, 1996, **211**, 147; (*i*) J. Wiorkiewicz-Kuczera and M. Karplus, *J. Am. Chem. Soc.*, 1990, **112**, 5324.

19 T. Fujii and T. Itaya, *Heterocycles*, 1999, **51**, 2255.

20 (*a*) J. C. Schwartz, A. P. Wade, C. G. Enke and R. G. Cooks, *Anal. Chem.*, 1990, **62**, 1809; (*b*) J. S. Patrick, T. Pradeep, H. Luo, S. Ma and R. G. Cooks, *J. Am. Soc. Mass Spectrom.*, 1998, **9**, 1158.

21 H. Deng and P. Kebarle, *J. Phys. Chem. A*, 1998, **102**, 571 and references cited therein.

22 (*a*) R. W. Vachet, J. A. R. Hartman and J. H. Callahan, *J. Mass Spectrom.*, 1998, **33**, 1209; (*b*) M. Y. Combariza and R. W. Vachet, *J. Am. Soc. Mass Spectrom.*, 2002, **13**, 813.

23 (*a*) B. A. Perera, M. P. Ince, E. R. Talaty and M. J. van Stipdonk, *Rapid Commun. Mass Spectrom.*, 2001, **15**, 615; (*b*) J. L. Seymour and F. Turecek, *J. Mass Spectrom.*, 2000, **35**, 566; (*c*) J. R. Scott, G. S. Groenewold, A. K. Gianotto, M. T. Benson and J. B. Wright, *J. Phys. Chem. A*, 2000, **104**, 7079.

24 (*a*) J. El Nakat, K. J. Fisher, I. G. Dance and G. D. Willett, *Inorg. Chem.*, 1993, **32**, 1931; (*b*) M. N. Yi, K. Fisher and I. Dance, *New J. Chem.*, 2001, **25**, 73.

25 (*a*) E. Sletten, *Acta Crystallogr., Sect. B*, 1969, **25**, 1480; (*b*) E. Sletten, *Acta Crystallogr., Sect. B*, 1970, **26**, 1609; (*c*) P. de Meester and A. C. Skapski, *J. Chem. Soc. A*, 1971, 2167; (*d*) A. Terzis, A. L. Beauchamp and R. Rivest, *Inorg. Chem.*, 1973, **12**, 1166.

26 (*a*) P. de Meester, S. R. Fletcher and A. C. Skapski, *J. Chem. Soc., Dalton Trans.*, 1973, 2575; (*b*) R. G. Griffin, J. D. Ellett Jr., M. Mehring, J. G. Bullitt and J. S. Waugh, *J. Chem. Phys.*, 1972, 2147; (*c*) D. Lawton and R. Mason, *J. Am. Chem. Soc.*, 1965, **87**, 921.

27 Part 32. J. M. Farrugia and R. A. J. O'Hair, *Int. J. Mass Spectrom.*, in press.